

**Biophysical Journal, Volume 112**

**Supplemental Information**

**Rate-Dependent Role of  $I_{Kur}$  in Human Atrial Repolarization and Atrial Fibrillation Maintenance**

**Martin Aguilar, Jianlin Feng, Edward Vigmond, Philippe Comtois, and Stanley Nattel**

## SUPPORTING MATERIAL: FIGURE LEGENDS

**Figure S1.** Model inactivation and activation gating variables and time constants. (A) Inactivation gating variable as a function of transmembrane potential ( $V_m$ ) for the original model ( $u_{i,original}$ ; blue) and fast ( $u_{i,f}$ , red solid) and slow ( $u_{i,s}$ , red dashed) inactivation gating variables for the modified model. (B) Inactivation time constants as a function of transmembrane potential for the original ( $\tau_{ui,original}$ , blue) and modified ( $\tau_{ui,f}$ , red solid;  $\tau_{ui,s}$ , red dashed) model. (C) Activation gating variable as a function of transmembrane potential for the original ( $u_{a,original}$ , blue) and modified ( $u_{a,modified}$ , red) model. (D) Activation time constant as a function of transmembrane potential for the original ( $\tau_{ua,original}$ , blue) and modified ( $\tau_{ua,modified}$ , red) model.

**Figure S2.**  $I_{Kur}$  inactivation and action potential dynamics. (A) Action potential amplitude (APA), (B) action potential duration at 90% repolarization (APD<sub>90</sub>), (C) maximal phase-0 overshoot potential (OS) and (D) peak Na<sup>+</sup> current (peak  $I_{Na}$ ) as a function of stimulation cycle length (CL) for the original (black) and modified (red) Courtemanche models.

**Figure S3.** Left panels: Kinetic determinants of  $I_{Kur}$  at a cycle length of 750 ms. Right panels: Cycle-length dependence of the same kinetic determinants (points corresponding to a cycle length of 750 ms indicated by an X). (A) Determinants of  $I_{Kur}$  rate dependence as a function of time for a stimulation cycle length (CL) of 750 ms. The area under the  $I_{Kur}$  curve ( $I_{Kur}$  AUC; shaded red) is calculated to determine charge carried per cycle. (B)  $I_{Kur}$  AUC as a function of stimulation cycle length. (C) Inactivation gate open probability ( $u_{i,f} \times u_{i,s}$ ) as a function of time at CL = 750 ms. The open-probability minimum is marked by a red dot. (D) Inactivation gate open probability minima as a function of cycle length. (E) Activation gate open probability ( $u_a^3$ ) as a function of time at CL = 750 ms. The area under the  $u_a^3$  curve ( $u_a^3$  AUC) is shaded in red. (F) Activation gate open probability AUC ( $u_a^3$  AUC) as a function of stimulation cycle length.

**Figure S4.** ACh distributions used for the 2-dimensional AF simulations. Pattern #1 is a flat ACh distribution. Pattern #2 and #3 are sinusoidal ACh distributions. Three peak ACh concentrations (1.875 nM, 3.75 nM and 7.5 nM) for each pattern generated 9 different substrate conditions.

**Figure S5.** Representative example of simulated cholinergic AF using pattern #1 with peak ACh concentration of 7.5 nM and the non-remodeled cardiomyocyte model. (A) ACh distribution with peak concentration of 7.5 nM and (B) corresponding APD<sub>60</sub> distribution. (C) Transmembrane potential over time at 50 ms intervals; re-entry is very stable and maintained by a single rotor. (D) Ratio of depolarized cells and (E) transmembrane potential over time for the cardiomyocyte marked with a white circle in panels A and B.

**Figure S6.** Representative example of simulated cholinergic AF using pattern #3 with peak ACh concentration of 7.5 nM and the non-remodeled cardiomyocyte model. (A) ACh distribution with peak concentration of 7.5 nM and (B) corresponding APD<sub>60</sub> distribution. (C) Transmembrane potential over time at 50 ms intervals; re-entry is maintained by multiple short-live spiral waves. (D) Ratio of depolarized cells and (E) transmembrane potential over time for the cardiomyocyte marked with a white circle in panels A and B.

**Figure S7.** Representative example comparing re-entry dynamics in the original and modified models. (A-B) Transmembrane potential over time at 50 ms intervals for the original and modified models. (C-D) APD<sub>-60</sub> for the original and modified models. (E-F) Ratio of depolarized cells and transmembrane potential for the original (blue) and modified (red) models. Non-remodeled cardiomyocyte model with ACh pattern #1 with peak concentration of 1.875 nM.

**Figure S8.** Representative example comparing re-entry dynamics in the original and modified models. (A-B) Transmembrane potential over time at 50 ms intervals for the original and modified models. (C-D) APD<sub>-60</sub> for the original and modified models. (E-F) Ratio of depolarized cells and transmembrane potential for the original (blue) and modified (red) models. Non-remodeled cardiomyocyte model with ACh pattern #3 with peak concentration of 3.75 nM.

**Figure S9.** Representative example of re-entry termination by 100% I<sub>Kur</sub> block using ACh pattern #2 with peak ACh concentration of 3.75 nM and the non-remodeled cardiomyocyte model. (A) ACh distribution with peak concentration of 3.75 nM and (B) corresponding APD<sub>-60</sub> distribution. (C) Transmembrane potential over time at 50 ms intervals; 50% I<sub>Kur</sub> block was introduced at  $t_{\text{drug}} = 1600$  ms. (D) Ratio of depolarized cells and (E) transmembrane potential over time for the cardiomyocyte marked with a white circle in panels A and B for control (blue) and 50% I<sub>Kur</sub> block (red).

**Figure S10.** Representative example of simulated cholinergic AF using pattern #1 with peak ACh concentration of 3.75 nM and the remodeled cardiomyocyte model. (A) ACh distribution with peak concentration of 3.75 nM and (B) corresponding APD<sub>-60</sub> distribution. (C) Transmembrane potential over time at 50 ms intervals; re-entry is very stable and maintained by a single rotor. (D) Ratio of depolarized cells and (E) transmembrane potential over time for the cardiomyocyte marked with a white circle in panels A and B.

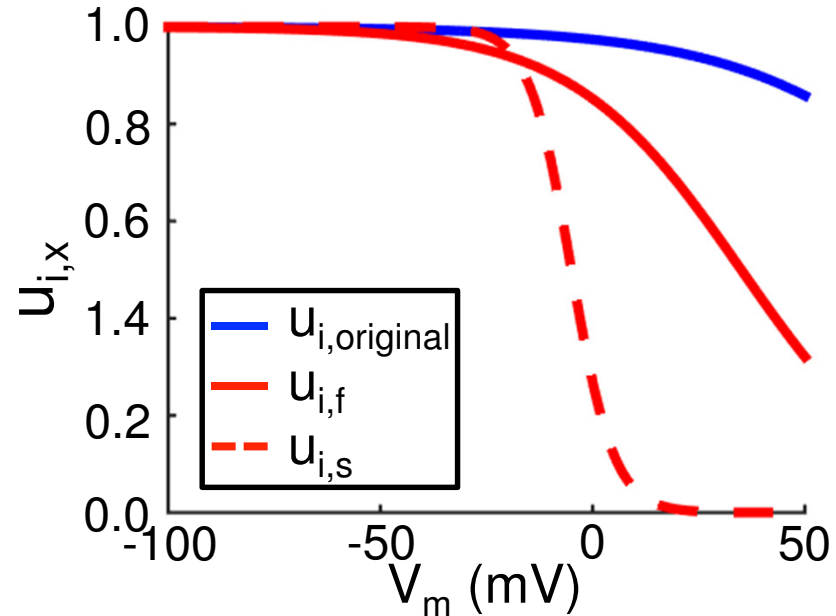
**Figure S11.** Representative example of simulated cholinergic AF using pattern #2 with peak ACh concentration of 3.75 nM and the remodeled cardiomyocyte model. (A) ACh distribution with peak concentration of 3.75 nM and (B) corresponding APD<sub>-60</sub> distribution. (C) Transmembrane potential over time at 50 ms intervals; re-entry is very stable and maintained by a single rotor. (D) Ratio of depolarized cells and (E) transmembrane potential over time for the cardiomyocyte marked with a white circle in panels A and B.

**Figure S12.** Representative example of simulated cholinergic AF using pattern #3 with peak ACh concentration of 3.75 nM and the remodeled cardiomyocyte model. (A) ACh distribution with peak concentration of 3.75 nM and (B) corresponding APD<sub>-60</sub> distribution. (C) Transmembrane potential over time at 50 ms intervals; re-entry is stable and maintained by a few rotors. (D) Ratio of depolarized cells and (E) transmembrane potential over time for the cardiomyocyte marked with a white circle in panels A and B.

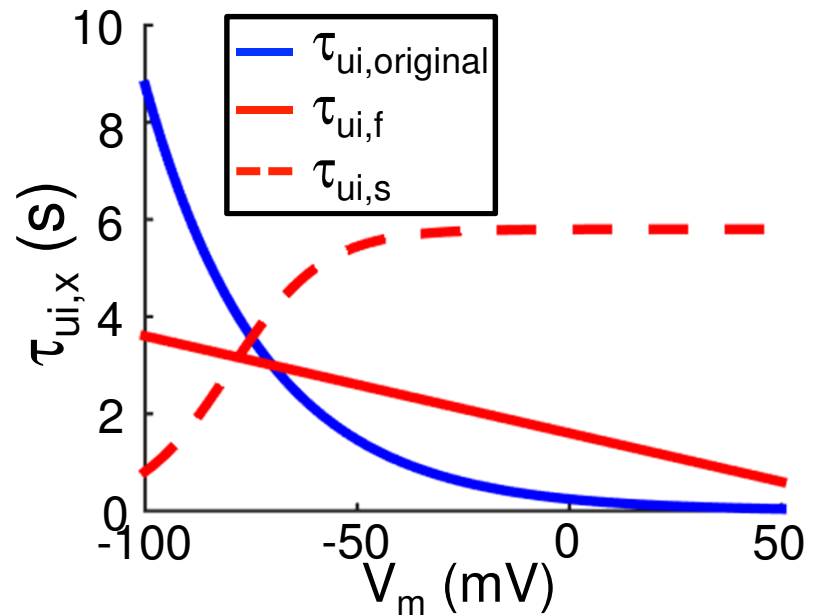
**Figure S13.** Representative example of re-entry non-termination by 100% I<sub>Kur</sub> block using ACh pattern #2 with peak ACh concentration of 3.75 nM and the remodeled cardiomyocyte model. (A) ACh distribution with peak concentration of 3.75 nM and (B) corresponding APD<sub>-60</sub> distribution. (C) Transmembrane potential over time at 50 ms intervals; 100% I<sub>Kur</sub> block was introduced at  $t_{\text{drug}} = 1000$  ms. (D) Ratio of depolarized cells and (E) transmembrane potential

over time for the cardiomyocyte marked with a white circle in panels A and B for control (blue) and 50%  $I_{Kur}$  block (red).

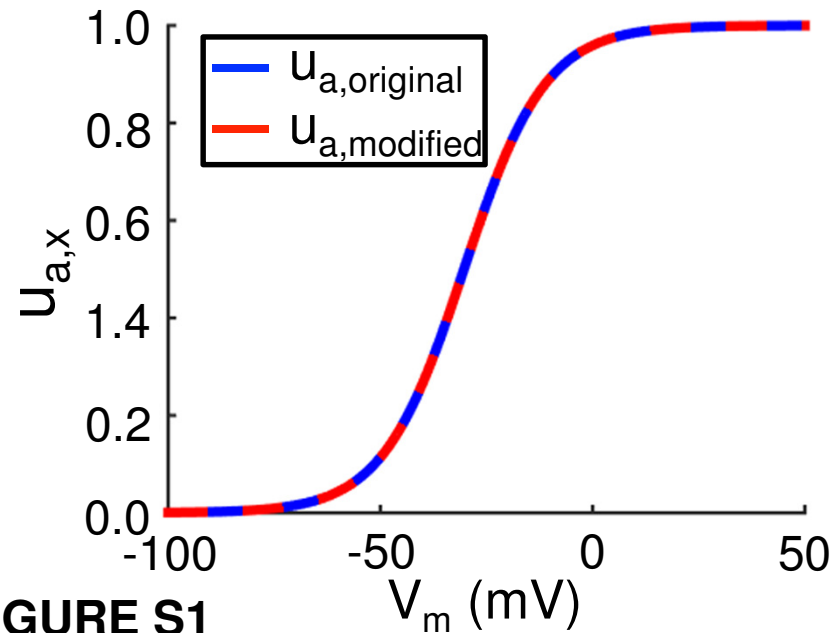
### A INACTIVATION GATING VARIABLES



### B INACTIVATION TIME CONSTANTS



### C ACTIVATION GATING VARIABLES



### D ACTIVATION TIME CONSTANTS

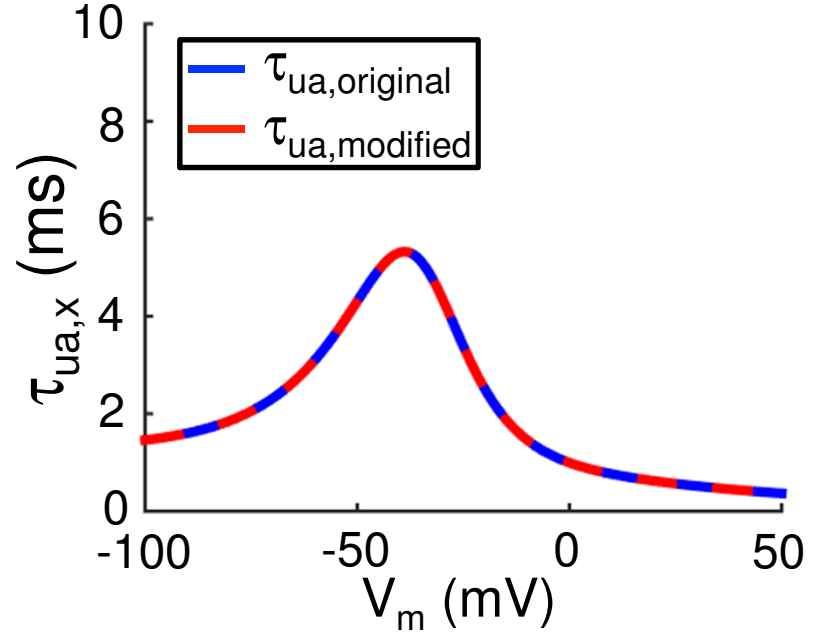
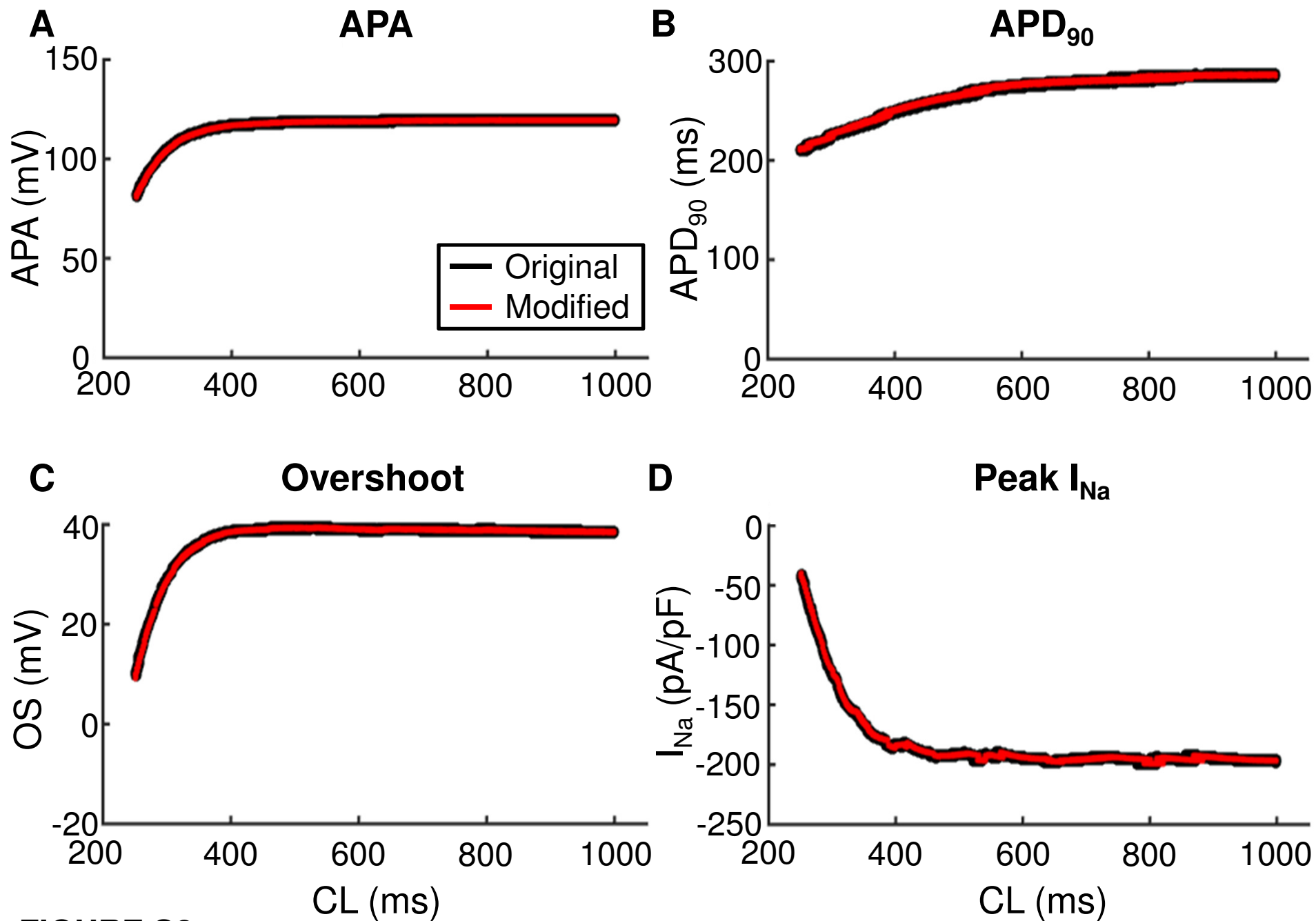


FIGURE S1



**FIGURE S2**

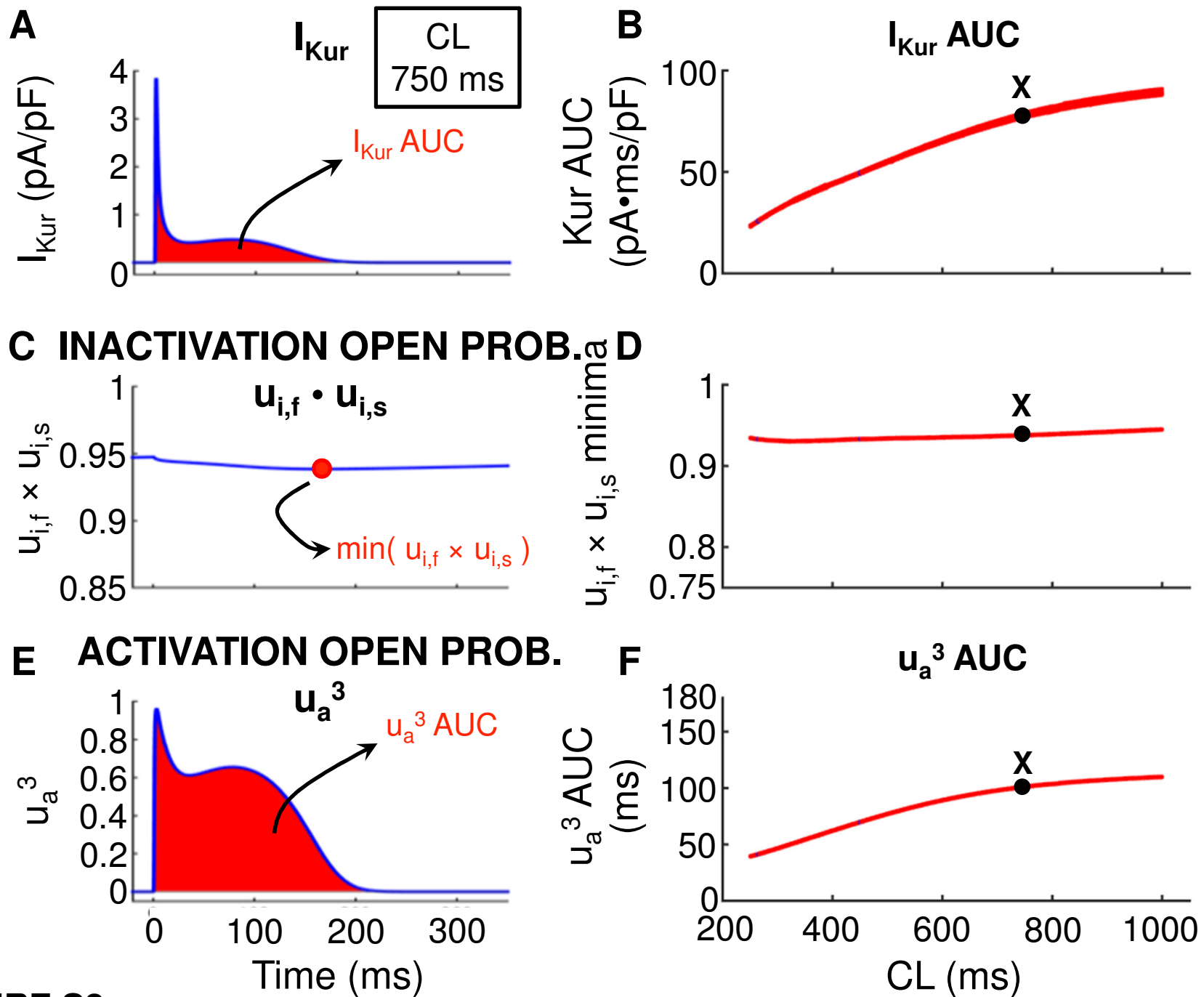
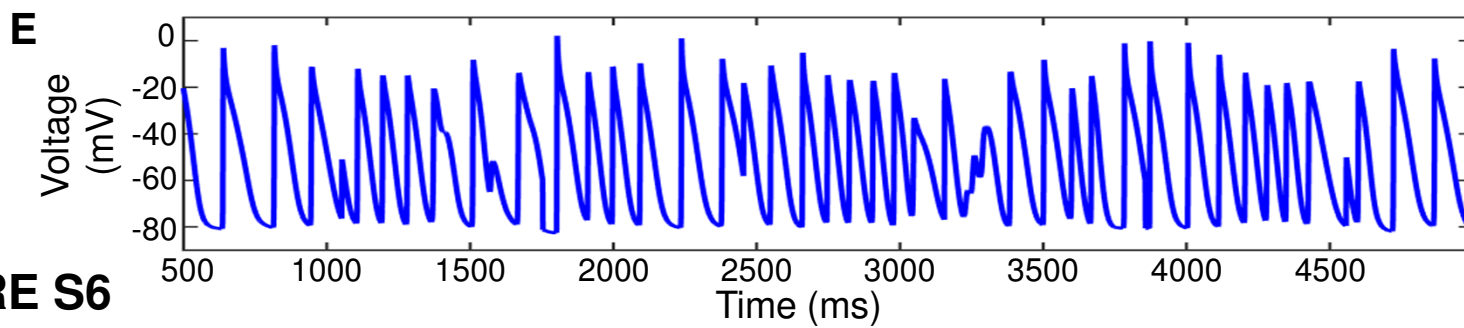
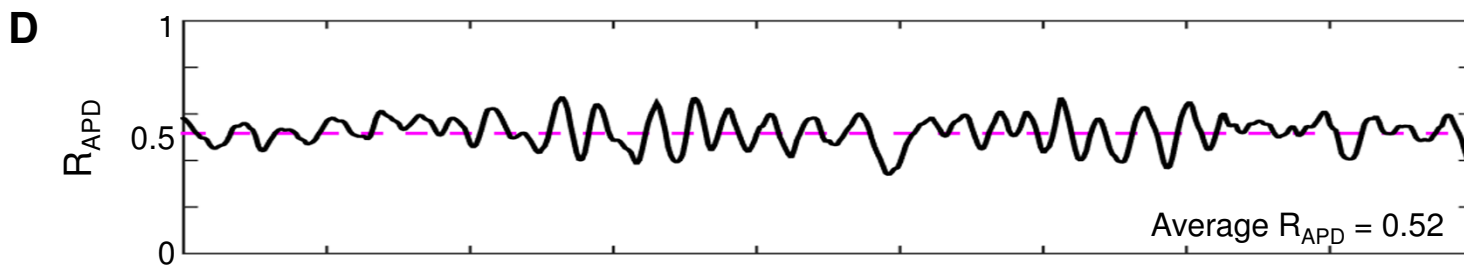
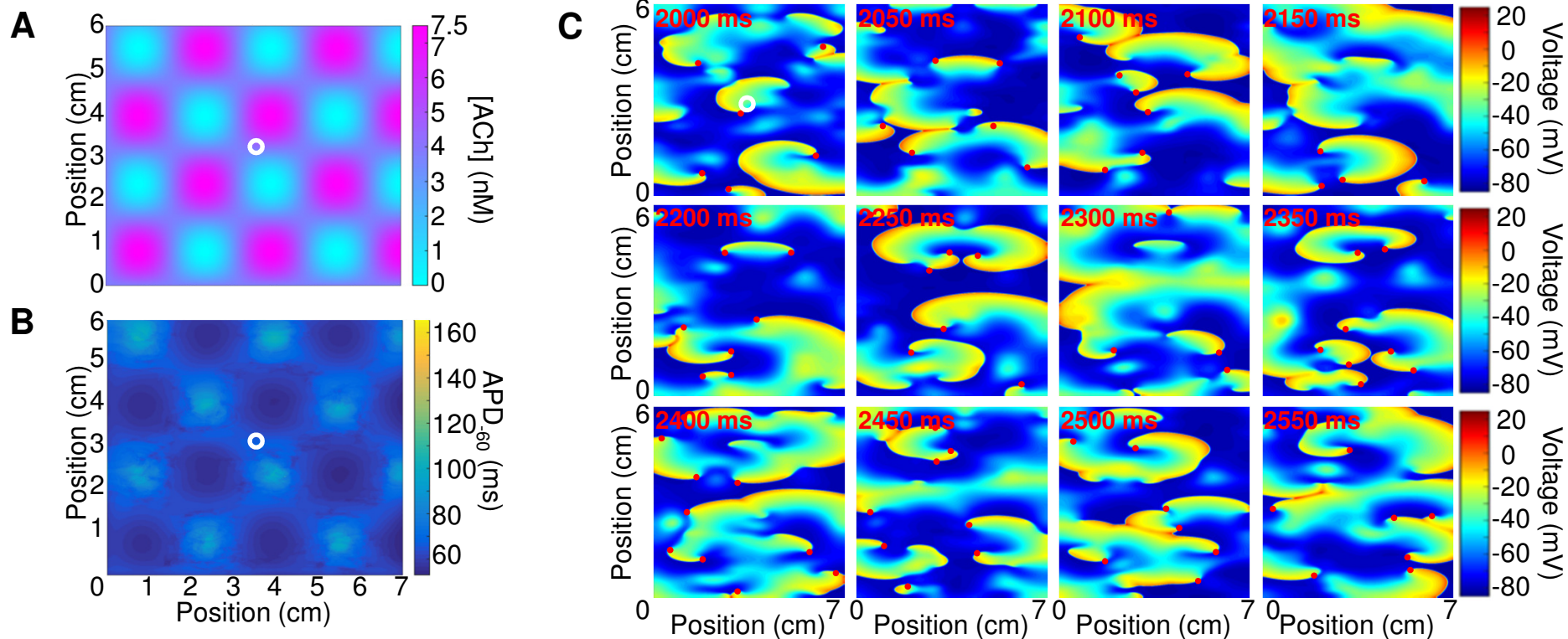


FIGURE S3

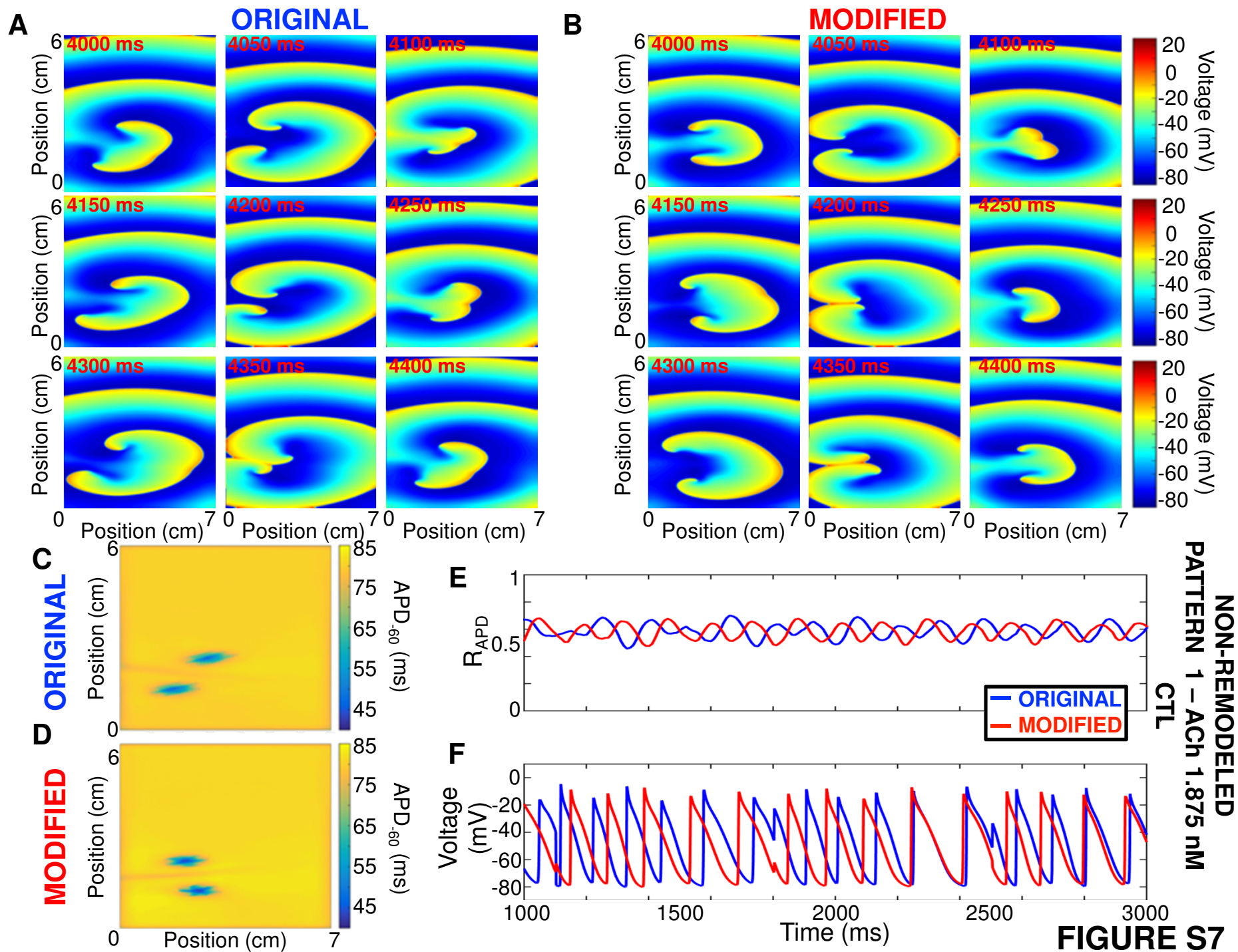






**NON-REMODELED  
 PATTERN 3  
 ACh 7.5 nM  
 CONTROL**

**FIGURE S6**



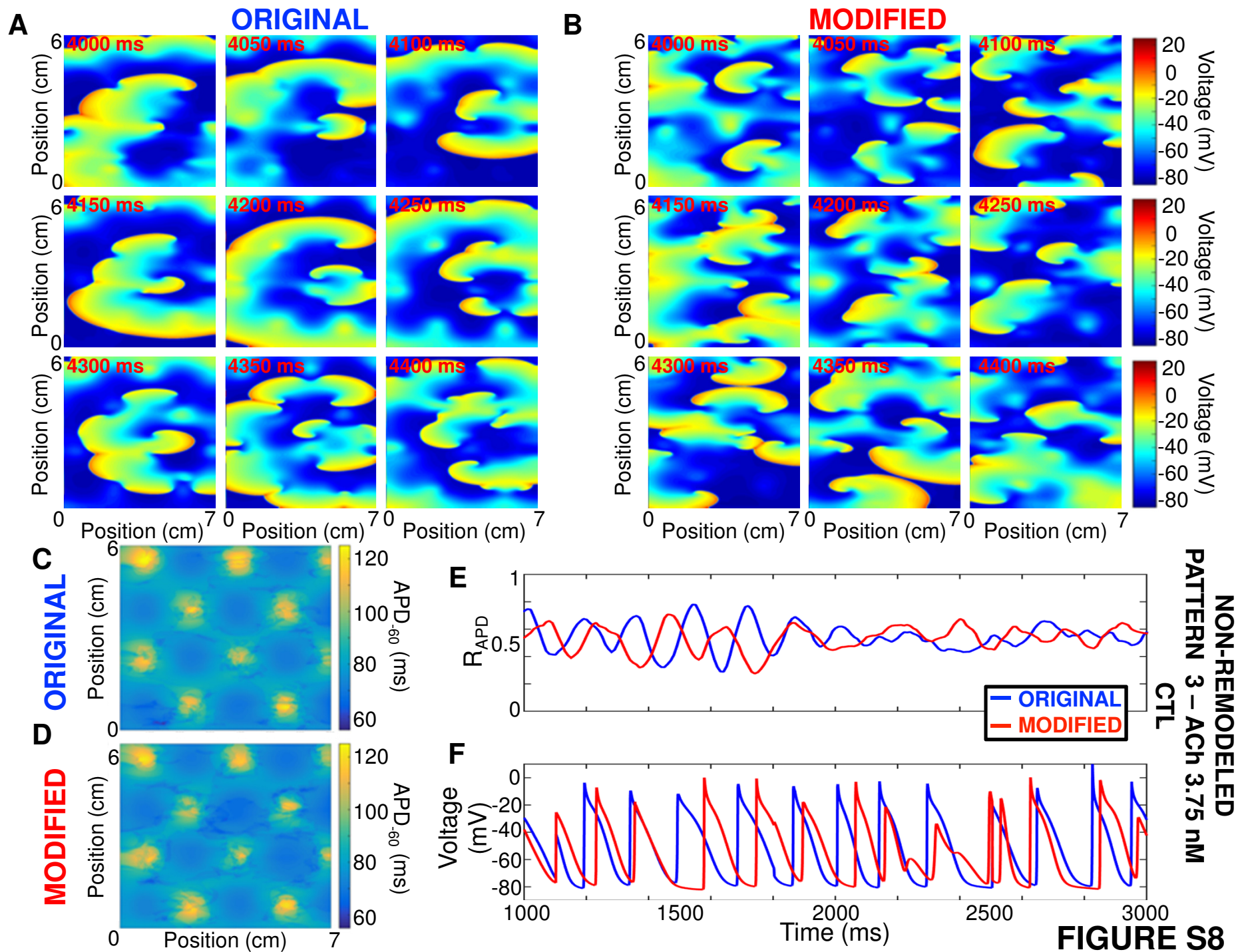


**FIGURE S8**

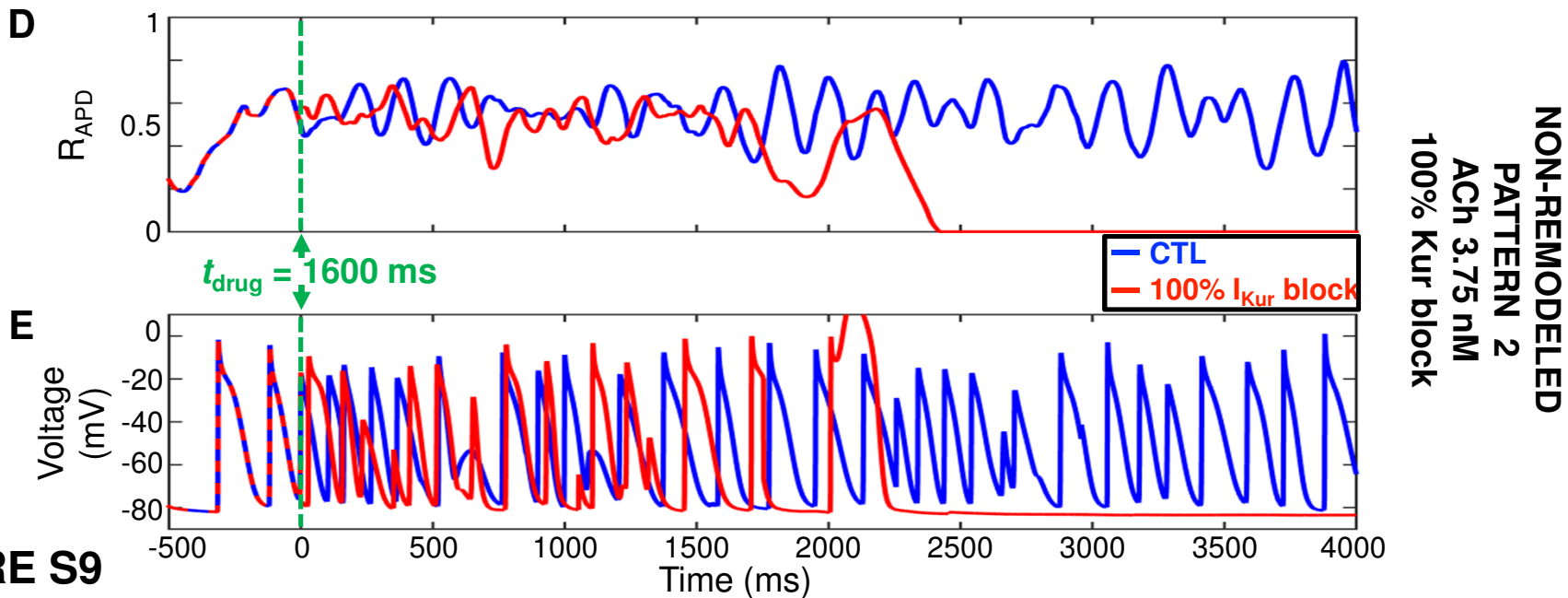
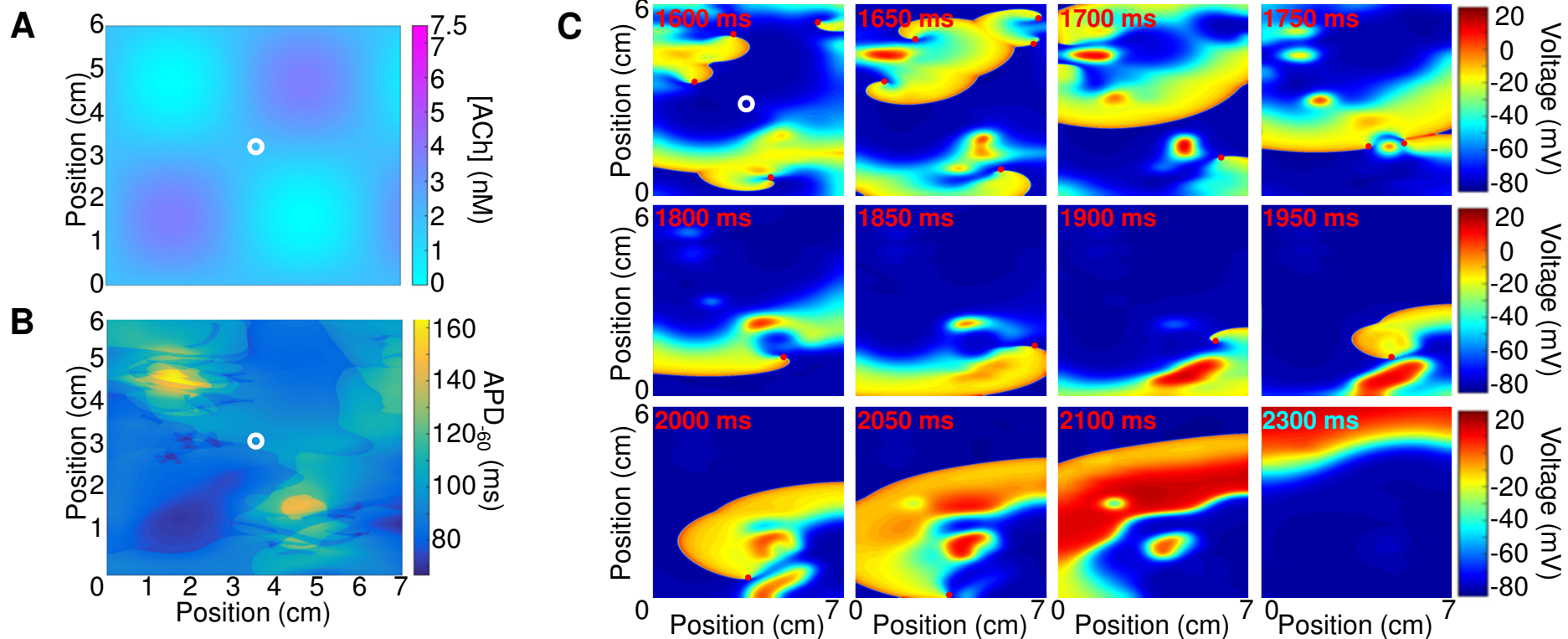
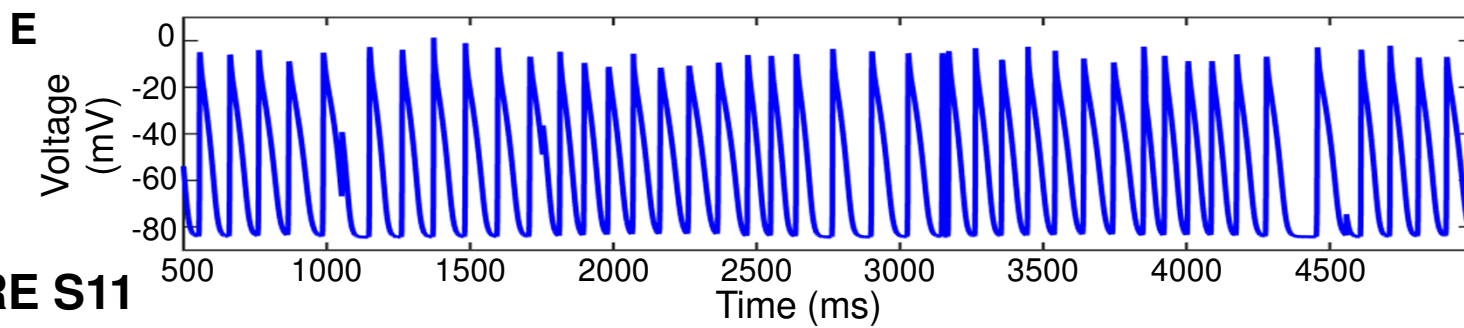
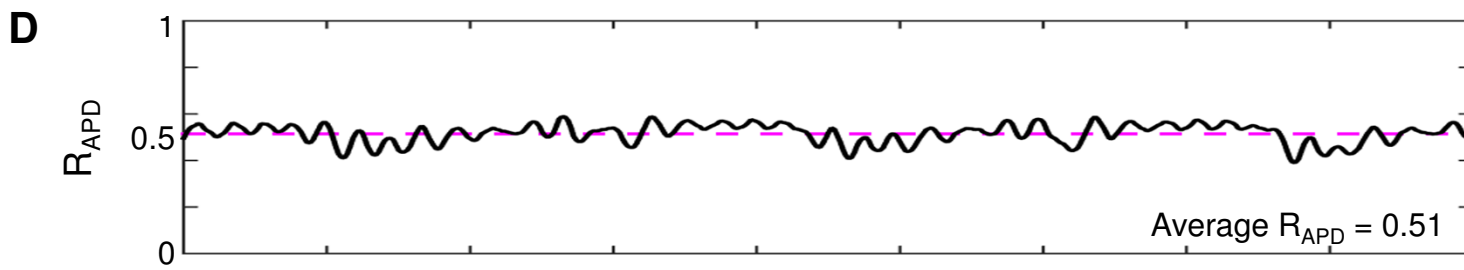
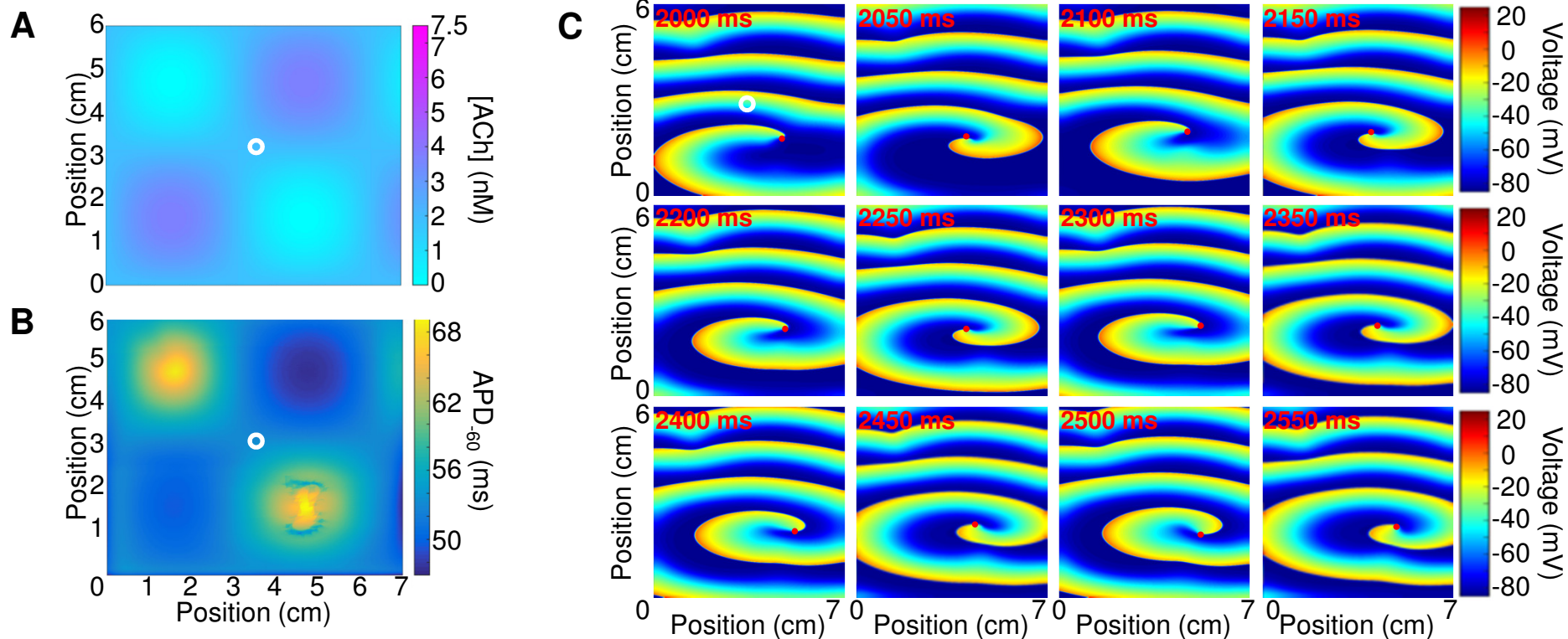


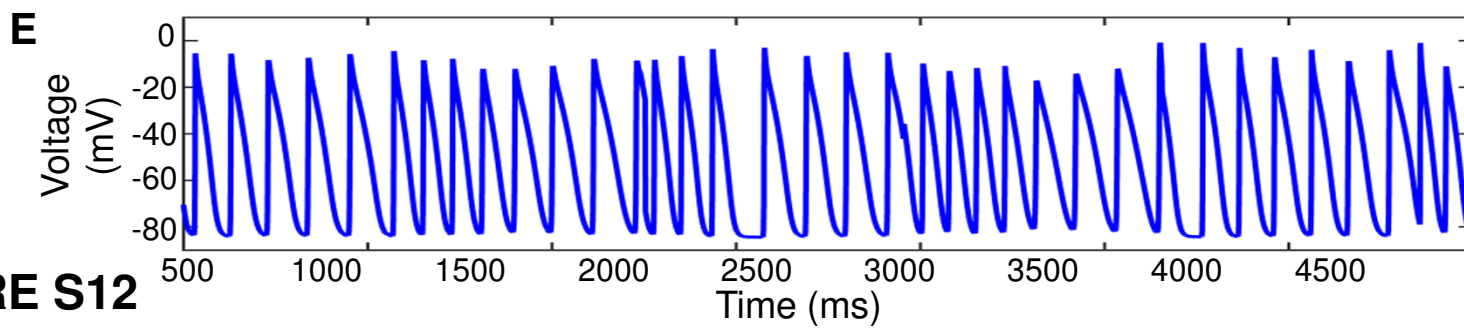
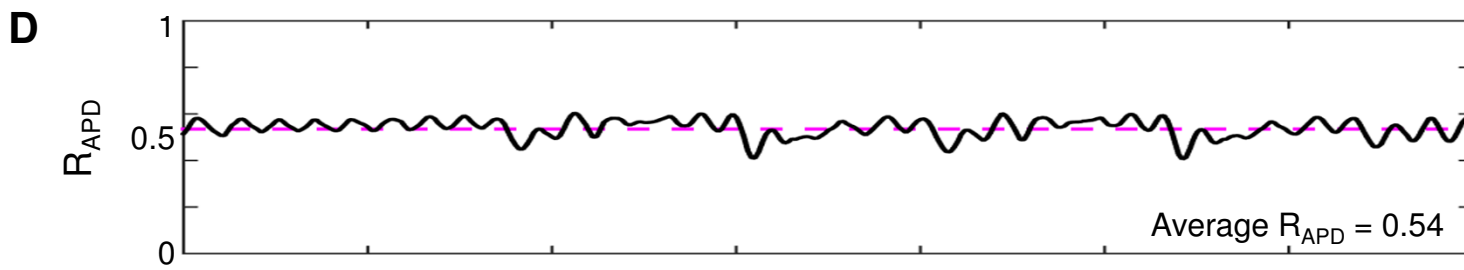
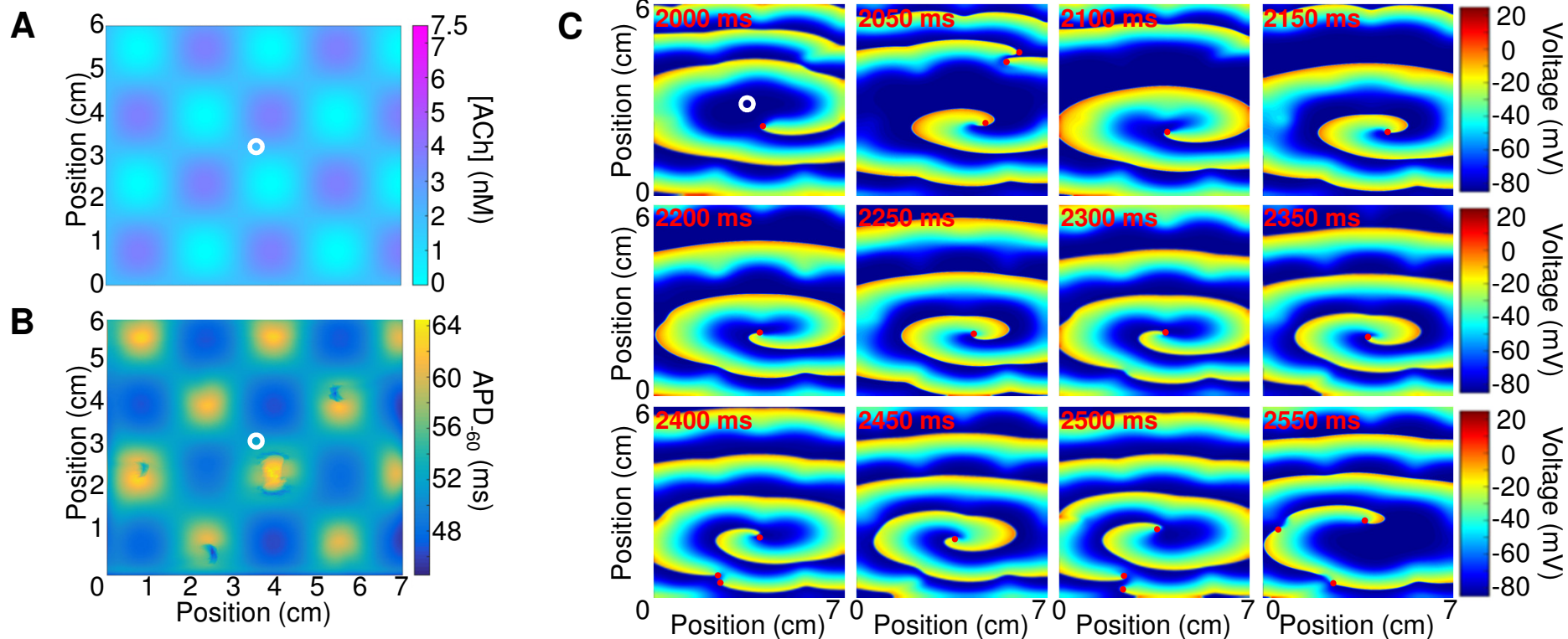
**FIGURE S9**





**REMODELED  
PATTERN 2  
ACh 3.75 nM  
CONTROL**

**FIGURE S11**



**REMODELED  
PATTERN 3  
ACh 3.75 nM  
CONTROL**

**FIGURE S12**

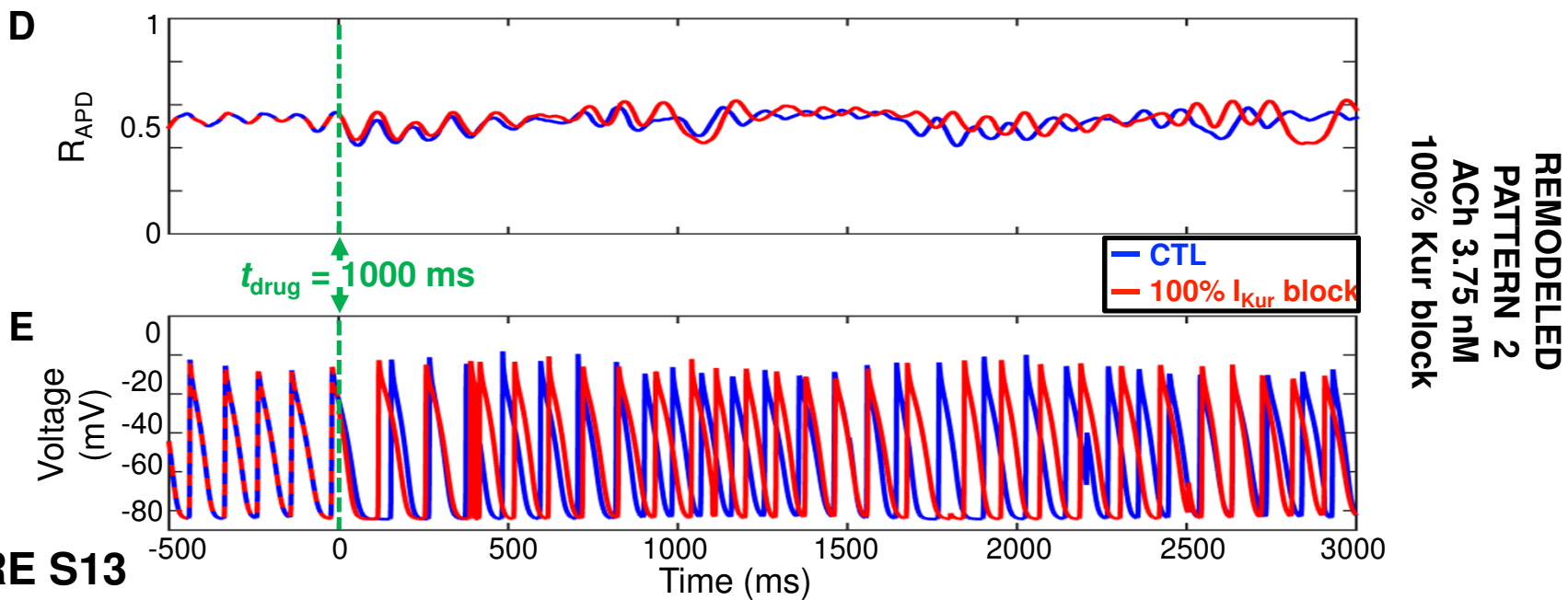
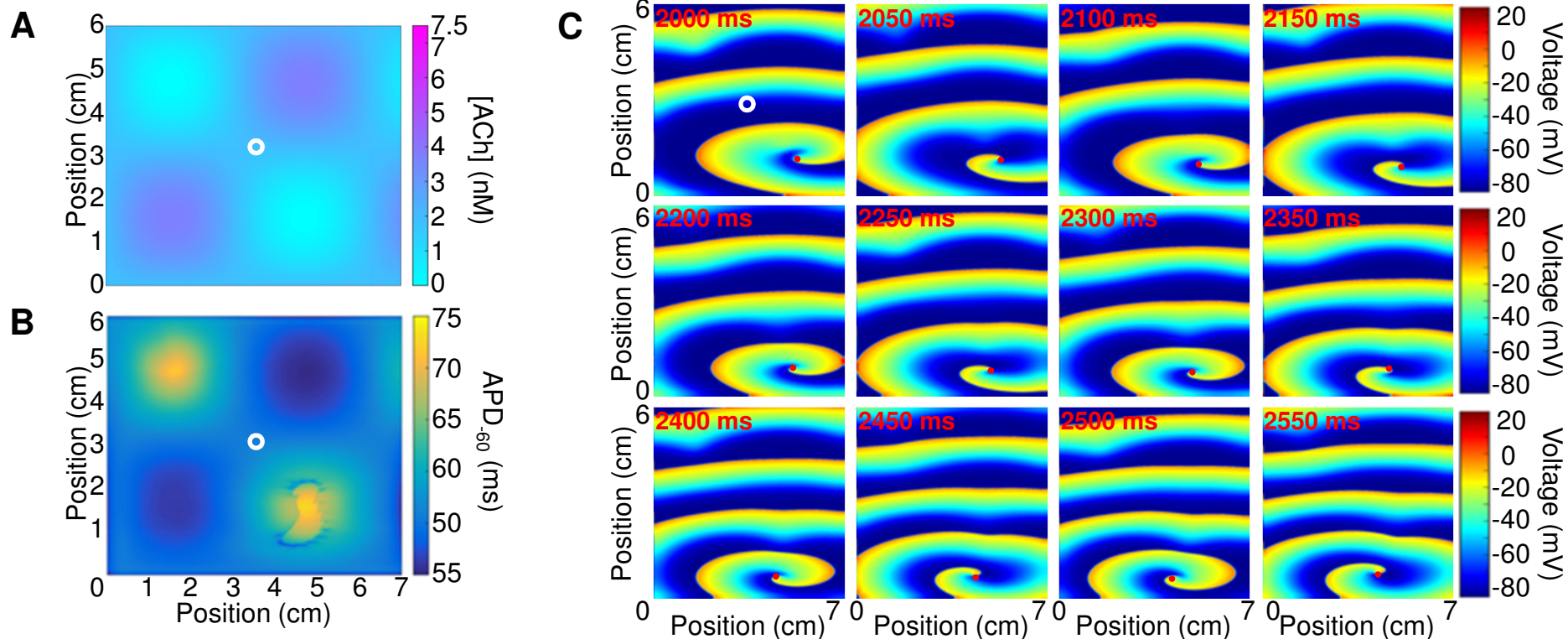


**FIGURE S13**